Commun. Comput. Phys.
doi: 10.4208/cicp.160412.111012a

Vol. **14**, No. 3, pp. 574-598
September 2013

Numerical Solution of Blow-Up Problems for Nonlinear Wave Equations on Unbounded Domains

Hermann Brunner[1,2], Hongwei Li[3,1,*] and Xiaonan Wu[1]

[1] *Department of Mathematics, Hong Kong Baptist University, Kowloon Tong, Hong Kong.*
[2] *Department of Mathematics and Statistics, Memorial University of Newfoundland, St. John's, NL, A1C 5S7, Canada.*
[3] *College of Mathematical Sciences, Shandong Normal University, Jinan, 250014, P.R. China.*

Received 16 April 2012; Accepted (in revised version) 11 October 2012

Available online 25 January 2013

Abstract. The numerical solution of blow-up problems for nonlinear wave equations on unbounded spatial domains is considered. Applying the unified approach, which is based on the operator splitting method, we construct the efficient nonlinear local absorbing boundary conditions for the nonlinear wave equation, and reduce the nonlinear problem on the unbounded spatial domain to an initial-boundary-value problem on a bounded domain. Then the finite difference method is used to solve the reduced problem on the bounded computational domain. Finally, a broad range of numerical examples are given to demonstrate the effectiveness and accuracy of our method, and some interesting propagation and behaviors of the blow-up problems for nonlinear wave equations are observed.

AMS subject classifications: 65M06, 65M20

Key words: Finite-time blow-up, nonlinear wave equation, absorbing boundary conditions, finite difference method, unbounded domains.

1 Introduction

This paper is devoted to studying the numerical solution of blow-up problems for the nonlinear wave equation of the form

$$u_{tt} = a^2 \Delta u + |u|^p, \quad x \in \Omega, \quad t > 0, \tag{1.1}$$

$$u(x,0) = \phi_0(x), \quad u_t(x,0) = \phi_1(x), \quad x \in \Omega, \tag{1.2}$$

*Corresponding author. *Email addresses:* hbrunner@math.hkbu.edu.hk, hermann@math.mun.ca (H. Brunner), lhwqust@gmail.com (H. Li), xwu@hkbu.edu.hk (X. Wu)

where $u(x,t)$ represents the wave displacement at position x and time t, Δ denotes the Laplacian, a is the given reference wave speed, $\phi_0(x)$ and $\phi_1(x)$ are the initial values, and the spatial domain Ω is given by $\Omega=\mathbb{R}^d$ $(d=1,2,\cdots)$. The wave equation appears in applications in various areas of mathematical physics. As an example, the blow-up problem would be that of the focusing energy-subcritical nonlinear wave equations with electromagnetic potential in electromagnetism [1] (For more applications see the list of the references in [2–4]).

The theory of finite-time blow-up for nonlinear wave equations has an interesting and exciting history. We will only give a brief summary and refer the reader to the papers [5–11] and the survey paper [12]. Strauss [5] conjectured that if the critical value, $p_0(d)$, is the positive root of $(d-1)x^2-(d+1)x-2=0$, then, if $1<p<p_0(d)$, the solution of the nonlinear wave equation blows up in finite time for any choice of the initial conditions. Glassey [6, 7] subsequently verified the conjecture in two dimensions by showing that $p_0(2)=\frac{1}{2}(3+\sqrt{17})$. Sideris proved in his PhD thesis that there exists blow-up in finite time for all $p>1$ when $d=1$, and he also proved in [8] the conjecture of Strauss in high dimensions by averaging the Riemann function in time. The papers [9–11] contain a systematic analysis of the life-span of classical solutions for nonlinear wave equations.

For semilinear parabolic PDEs (reaction-diffusion equations) arising as models in combustion theory, the theoretical and physical aspects of single-point blow-up versus total blow-up are well understood (see for example Bebernes and Eberly [13], Section 5.5, and Lacey [14]). However, analogous studies on the possible sets of blow-up points for nonlinear wave equations do to the best of our knowledge not exist.

The numerical analysis of the blow-up problems for nonlinear wave equations (1.1)-(1.2) has so far received little attention, see [15, 16] and their references. For the bounded computational domain case, there are only few papers studying the numerical solution of blow-up problems. Cho [4] gave a finite difference scheme and proposed a rule for time-stepping for blow-up solutions of the one-dimensional nonlinear wave equation. For unbounded computational domains, the difficulties in the numerical solution of the problem (1.1)-(1.2) include three parts: the nonlinearity, the unboundedness, and the multidimensionality. To deal with the nonlinearity, we use the idea of the unified approach which was introduced by Zhang *et al.* [17, 18]; the basic idea underlying the unified approach is the well-known time-splitting method. Xu *et al.* [19] designed absorbing boundary conditions for nonlinear Schrödinger equations by using the time-splitting method. The idea of time-splitting method was extended for solving two-dimensional sine-Gordon equation by Han *et al.* [20]. For unboundedness, one of the most popular approaches is the use of the absorbing boundary conditions (ABCs) method, which is a powerful method to reduce the problems on an unbounded domain to a bounded domain, for an appropriate bounded computational domain. For the multidimensional case, it is hard to find suitable absorbing boundary conditions at the corners of a rectangle; we construct the conditions of corners by the average of two artificial boundary conditions to overcome this difficulty.

How to select a suitable bounded computational domain and derive appropriate ab-

sorbing boundary conditions on the artificial boundaries is a challenge, since we expect that the ABCs not only be easy to implement, but also imitate the perfect absorption of waves traveling out of the bounded domain through the artificial boundary. Many mathematicians, engineers and physicists have well developed the artificial boundary method for more than three decades. Higdon [21] proposed the high order local absorbing boundary conditions for linear wave equation. For a detailed account of artificial boundary method, the interested reader should consult [22–27] and the references therein. In recent years, there has been some new progress on the artificial boundary method for nonlinear partial differential equations (PDEs) on unbounded domains, see the papers [28–33] and the review [34]. However, as we all know, there are only few papers to study the numerical simulation of blow-up problems for semilinear parabolic PDEs on unbounded domains. Brunner and his co-workers [35,36] proposed the nonlinear absorbing boundary conditions for the one-dimensional and two-dimensional cases and gave an efficient adaptive time-stepping scheme. Zhang *et al.* [37] studied the numerical blow-up of semilinear parabolic PDEs on unbounded domains, derived the nonlinear absorbing boundary conditions, and employed an adaptive time-stepping scheme.

In general, the absorbing boundary conditions can be classified into nonlocal ABCs (also called global ABCs) and local ABCs. The nonlocal ABCs are usually expensive for practical simulations, since the nonlocal ABCs try to simulate the effect of the exterior in an exact sense and are fully coupled in space and time; while the local ABCs are local in both space and time, which are computationally efficient and tractable. In order to save the computational cost, we are concerned with the construction of local ABCs and the numerical solution of the blow-up problem for the nonlinear wave equation on the unbounded domain in this paper.

The rest of this paper is organized as follows. In Section 2 we review the unified approach and the local absorbing boundary conditions for the linear wave equation, and use them to construct the nonlinear local absorbing boundary conditions for the nonlinear wave equation. Consequently, we obtain an initial-boundary-value problem on the bounded computational domain. Section 3 presents a discretization scheme for the resulting initial-boundary-value problem. Numerical examples are shown in Section 4 to confirm our theoretic analysis. In the practical computations, we observe the interesting phenomenon that the number of the blow-up points are different for different initial conditions or nonlinear terms. Finally, some conclusions are drawn in Section 5.

2 Nonlinear local absorbing boundary conditions

In this section, we first review the idea underlying the unified approach and the local absorbing boundary conditions for the linear wave equation, and then combine these methods to design nonlinear local absorbing boundary conditions for the nonlinear wave equation.

2.1 Review of unified approach

The well-known time-splitting method is a powerful approach for the numerical simulation of complex physical time-dependent models. Based on the time-splitting method, the basic idea of the unified approach is to distinguish between incoming and outgoing waves along the boundaries for the linear subproblem, and to approximate the corresponding linear operator by using a 'one-way operator' (to make waves outgoing), then the approximate operator and the nonlinear subproblem is united to yield the nonlinear boundary conditions.

We concentrate on analyzing the two-dimensional case. Extending the idea underlying the unified approach, we now aim to design the nonlinear local ABCs of Eq. (1.1). We assume $v=u_t$, and define the vector function $U=[u,v]^T$. Then Eq. (1.1) can be equivalently written in the operator form

$$U_t \equiv (u_t, v_t)^T = \mathbf{L}U + \mathbf{N}U, \tag{2.1}$$

where $\mathbf{L}$ represents the linear operator, and $\mathbf{N}$ represents the nonlinear operator that governs the effect of the nonlinearity. The operators are given by

$$\mathbf{L}U := \begin{pmatrix} v \\ a^2\Delta u \end{pmatrix} \quad \text{and} \quad \mathbf{N}U := \begin{pmatrix} 0 \\ |u|^p \end{pmatrix}. \tag{2.2}$$

The time-splitting approach means that the wave propagation carries out the action of a kinetic energy step and a potential energy step separately for a small time size τ. Hence, using the operator splitting in a time interval from t to $t+\tau$ for small τ, we obtain

$$U(x,t+\tau) \approx e^{(\mathbf{L}+\mathbf{N})\tau} U(x,t), \tag{2.3}$$

in analogy to the well-known Strang splitting [38]

$$U(x,t+\tau) \approx e^{\mathbf{L}\tau/2} e^{\mathbf{N}\tau} e^{\mathbf{L}\tau/2} U(x,t). \tag{2.4}$$

First of all, making the wave outgoing of the computational domain, we derive the approximate operator $\tilde{\mathbf{L}}$ for the linear operator $\mathbf{L}$, then replace the operator $\mathbf{L}$ in (2.3). By restricting to the artificial boundaries and letting τ tend to zero, we have the one-way equation

$$U_t = \tilde{\mathbf{L}}U + \mathbf{N}U. \tag{2.5}$$

Once we obtain the approximation operator, Eq. (2.5) takes the role of the nonlinear local ABCs. The difficulty is how to design a good approximation operator $\tilde{\mathbf{L}}$ for the linear operator $\mathbf{L}$. The derivation of the operator $\tilde{\mathbf{L}}$ is explained in the coming subsection.

2.2 Local absorbing boundary conditions for the linear wave equation

In this subsection we recall the construction of local ABCs for the linear wave equation

$$u_{tt}=a^2\Delta u, \tag{2.6}$$

which is equivalent to the operator form

$$U_t\equiv(u_t,v_t)^T=\mathbf{L}U. \tag{2.7}$$

In the frequency domain, Eq. (2.6) implies the dispersion relation

$$\omega^2=a^2(\xi^2+\eta^2), \tag{2.8}$$

where ω is the time frequency, and ξ and η are the wave numbers in the x direction and the y direction, respectively. To make the wave outgoing, one solves Eq. (2.8) to find

$$a\xi=\pm\omega\sqrt{1-\frac{a^2\eta^2}{\omega^2}}, \tag{2.9}$$

where the positive sign in (2.9) corresponds to the dispersion relation on the east boundary, and the negative sign in (2.9) corresponds to the one on the west boundary. The exact absorbing boundary conditions can be obtained by transforming the dispersion equation (2.9) into the space-time domain. However, it can not be implemented in space-time coordinates, since the inverse transformation of the square-root term in (2.9) results in a pseudo-differential operator that can not be implemented using numerical methods. Naturally, by approximating the square-root in (2.9) and using the duality $\xi\Leftrightarrow-i\partial_x$, $\eta\Leftrightarrow-i\partial_y$ and $\omega\Leftrightarrow i\partial_t$ between the frequency and physical domains, some local ABCs can be obtained [22,23].

In [21,24], Higdon proposed the following local ABCs on the east boundary:

$$\prod_{l=1}^{r}\Big(\cos\theta_l\partial_t+a\partial_x\Big)u=0. \tag{2.10}$$

Here r is an integer and $\pm\theta_l$ $(l=1,2,\cdots,r)$ are the angles between the wave incident direction and the normal direction of the boundary (here $|\theta_l|<\frac{\pi}{2}$ for all l).

In the practical numerical simulation, it is expensive to calculate the high-order derivatives for very large r; instead, we simply select $r=2$. On the east boundary we have

$$\cos\theta_1\cos\theta_2u_{tt}+a(\cos\theta_1+\cos\theta_2)u_{xt}+a^2u_{xx}=0. \tag{2.11}$$

Using the assumption $v=u_t$ and setting

$$S=\begin{pmatrix}1 & 0\\ a(\cos\theta_1+\cos\theta_2)\partial_x & \cos\theta_1\cos\theta_2\end{pmatrix},$$

Eq. (2.11) can be equivalently rewritten as

$$U_t = S^{-1}\begin{pmatrix} v \\ -a^2 u_{xx} \end{pmatrix} \equiv \tilde{\mathbf{L}}U. \tag{2.12}$$

Combining Eq. (2.7) with Eq. (2.12), we obtain the approximation operator $\tilde{\mathbf{L}}$ for the operator $\mathbf{L}$, namely

$$\mathbf{L} \approx \tilde{\mathbf{L}} := S^{-1}\begin{pmatrix} 0 & 1 \\ -a^2\partial_x^2 & 0 \end{pmatrix}. \tag{2.13}$$

By the same argument, we can achieve the corresponding approximation operator $\tilde{\mathbf{L}}$ on the other artificial boundaries from the corresponding west, north and south local ABCs, which are respectively governed by

$$\begin{aligned}
&\cos\theta_1\cos\theta_2 u_{tt} - a(\cos\theta_1+\cos\theta_2)u_{xt} + a^2 u_{xx} = 0,\\
&\cos\theta_1\cos\theta_2 u_{tt} + a(\cos\theta_1+\cos\theta_2)u_{yt} + a^2 u_{yy} = 0,\\
&\cos\theta_1\cos\theta_2 u_{tt} - a(\cos\theta_1+\cos\theta_2)u_{yt} + a^2 u_{yy} = 0.
\end{aligned}$$

For other strategies to construct the local ABCs for nonlinear wave equation, see the papers [22, 28] and the references therein.

2.3 Local absorbing boundary conditions for the nonlinear wave equation

In this subsection, we construct the local ABCs for the nonlinear wave equation (1.1)-(1.2). For the sake of simplicity, we only discuss the derivation of the local absorbing boundary condition on the east boundary in detail. Recalling Eq. (2.1) in the procedure of the unified approach and the approximation operator $\tilde{\mathbf{L}}$ of (2.13), we obtain the one-way equation

$$U_t = \tilde{\mathbf{L}}U + \mathbf{N}U. \tag{2.14}$$

Multiplying the operator S to Eq. (2.14) and using the relation $v = u_t$, we arrive at the local absorbing boundary condition of the nonlinear wave equation on the east boundary:

$$\cos\theta_1\cos\theta_2 u_{tt} + a(\cos\theta_1+\cos\theta_2)u_{xt} + a^2 u_{xx} - \cos\theta_1\cos\theta_2|u|^p = 0. \tag{2.15}$$

Similarly, we obtain the corresponding local ABCs on the west, north and south boundary, respectively,

$$\cos\theta_1\cos\theta_2 u_{tt} - a(\cos\theta_1+\cos\theta_2)u_{xt} + a^2 u_{xx} - \cos\theta_1\cos\theta_2|u|^p = 0. \tag{2.16}$$

$$\cos\theta_1\cos\theta_2 u_{tt} + a(\cos\theta_1+\cos\theta_2)u_{yt} + a^2 u_{yy} - \cos\theta_1\cos\theta_2|u|^p = 0, \tag{2.17}$$

$$\cos\theta_1\cos\theta_2 u_{tt} - a(\cos\theta_1+\cos\theta_2)u_{yt} + a^2 u_{yy} - \cos\theta_1\cos\theta_2|u|^p = 0. \tag{2.18}$$

Coupling these local ABCs (2.15)-(2.18) with the nonlinear wave equation (1.1)-(1.2), we have the reduced initial-boundary-value problem (IBVP) on the bounded computational domain, which can be solved by the finite difference or finite element method.

We conclude this section with a brief remark on the *stability* of the reduced IBVP with the local ABCs on the bounded computational domain. According to the design of the local ABCs, the local ABCs annihilate only the energy arising in the bounded domain. It will not propagate energy from the exterior domain into the interior domain. Therefore, the perturbation appearing in the artificial boundaries will not affect the interior solution, and the obtained local ABCs are stable and efficient. The numerical results are presented in Section 4 demonstrate the stability and efficiency of the proposed local ABCs. For more a relevant discussion of this issue, see [36,37].

3 Difference scheme

In this section, we consider the reduced IBVP on the bounded computational domain $\Omega_i=[x_w,x_e]\times[y_s,y_n]$. We divide the bounded domain Ω_i by the uniform grids, and choose $h_x=(x_w-x_e)/J$ and $h_y=(y_s-y_n)/K$ for the grid sizes in space, where J and K are two positive integers.

The grid points are given by

$$\Omega_i=\left\{(x_j,y_k,t_n)|x_j=x_w+jh,y_k=y_n+kh,\ t_n=n\Delta t,\ j=0,\cdots,J,\ k=0,\cdots,K,\ n=0,\cdots,\right\}.$$

Denote the operators $D_\cdot^+$, $D_\cdot^-$ and $D_\cdot^0$ by forward, backward and centered differences in x, y and t directions, respectively. $S_\cdot^0$ represents centered sums, for example, $S_t^0u_{j,k}^n=(u_{j,k}^{n+1}+u_{j,k}^{n-1})/2$. $u_{j,k}^n$ represents the numerical approximation of the wave function u at the grid point (x_j,y_k,t_n), where t_n is the time-level and Δt is the time-step.

First of all, from time $t=t_{n-1}$ to time $t=t_{n+1}$, where $t_{n+1}=t_n+\Delta t$, $t_0=0$, we discretize Eq. (1.1) at the points (x_j,y_k,t_n) in the interior domain Ω_i and obtain

$$D_t^+D_t^-u_{j,k}^n=a^2\left(D_x^+D_x^-S_t^0u_{j,k}^n+D_y^+D_y^-S_t^0u_{j,k}^n\right)+|u_{j,k}^n|^p,$$

where $1\le j\le J-1$, $1\le k\le K-1$.

Then we discuss the discretized forms on the artificial boundaries and the corners. For the sake of simplicity, we only give the discretized difference schemes on the east boundary and the east-north corner. The local ABC (2.15) on the east boundary can be discretized by

$$\begin{aligned}&a(\cos\theta_1+\cos\theta_2)D_x^0D_t^0u_{J-1,k}^n+\cos\theta_1\cos\theta_2D_t^+D_t^-u_{J-1,k}^n\\&\quad+a^2D_x^+D_x^-S_t^0u_{J-1,k}^n-\cos\theta_1\cos\theta_2|u_{J-1,k}^n|^p=0,\end{aligned}\tag{3.1}$$

where $1\le k\le K-1$.

For the corner point (J,K), the corresponding discretized scheme has the form

$$\begin{aligned}&a(\cos\theta_1+\cos\theta_2)D_x^0D_t^0u_{J-1,K}^n+\cos\theta_1\cos\theta_2D_t^+D_t^-u_{J-1,K}^n+a^2D_x^+D_x^-S_t^0u_{J-1,K}^n\\&\quad+a(\cos\theta_1+\cos\theta_2)D_y^0D_t^0u_{J,K-1}^n+a^2D_y^+D_y^-S_t^0u_{J,K-1}^n+\cos\theta_1\cos\theta_2D_t^+D_t^-u_{J,K-1}^n\\&\quad-\cos\theta_1\cos\theta_2|u_{J-1,K}^n|^p-\cos\theta_1\cos\theta_2|u_{J,K-1}^n|^p=0.\end{aligned}\tag{3.2}$$

By the same procedure, the discretization of the other three boundary conditions and the corners can be obtained.

For other strategies to discretize the local ABCs on the corners, see the paper [39] and the references therein.

4 Numerical results

From the derivation of the local ABCs for the two-dimensional nonlinear wave equation, we can easily obtain the corresponding local ABCs by (2.15) and (2.16) for the one-dimensional case. In order to illustrate the performance of our proposed method, we now present some numerical examples. In the calculations, we choose the reference wave speed $a=1.0$. Through numerical experiments, we find that if one simply chooses $r=2$, $\theta_1=\pi/3$ and $\theta_2=0$, the given method is nearly transparent for the wave propagation. Compare also the remark in Section 5.

4.1 The one-dimensional case

In this subsection, we consider the one-dimensional nonlinear wave equation of the form

$$\begin{aligned}&u_{tt}=u_{xx}+|u|^p,\quad x\in\Omega,\quad t>0,\\&u(x,0)=\phi_0(x),\quad u_t(x,0)=\phi_1(x),\quad x\in\Omega.\end{aligned}$$

4.1.1 Blow-up phenomena

Example 4.1. We consider the nonlinear wave equation with the parameter of nonlinear term $p=2$ and different initial conditions.

The bounded computational domain is $0\le x\le 1$, and we set $\Delta t=0.2h$. The computation stops when $\max(u)$ attains $1.0e6$, $T_b(\Delta t,h)$ is the numerical blow-up time. From Table 1, we can see that $T_b(\Delta t,h)$ has a limit as $\Delta t\to 0$ when $h=\Delta t/0.2$. This example illustrates the dependence of the numerical blow-up time on the spatial mesh size.

Example 4.2. The parameter of nonlinear term is $p=2$, and the initial functions are given by

$$\phi_0(x)=30\sin(\pi x),\quad \phi_1(x)=0.$$

The bounded computational domain is $0\le x\le 1$.

Table 1: $T_b(\Delta t,h)$ with different initial data.

	$\phi_0(x)=300\sin(\pi x)$, $\phi_1(x)=0$	$\phi_0(x)=500\sin(\pi x)$, $\phi_1(x)=20\sin(2\pi x)$
Mesh	$T_b(\Delta t,h)$	$T_b(\Delta t,h)$
$h=1/128$	0.175000	0.134375
$h=1/256$	0.172656	0.132813
$h=1/512$	0.171484	0.132031
$h=1/1024$	0.170898	0.131641
$h=1/2048$	0.170801	0.131348
$h=1/4096$	0.170654	0.131250

Fig. 1 shows the evolution of $u(x,t)$ in time until $\max(u)$ reaches $1.2e4$. We choose this example to compare our method with the results obtained in [4]; our results show that they are similar to the ones in [4].

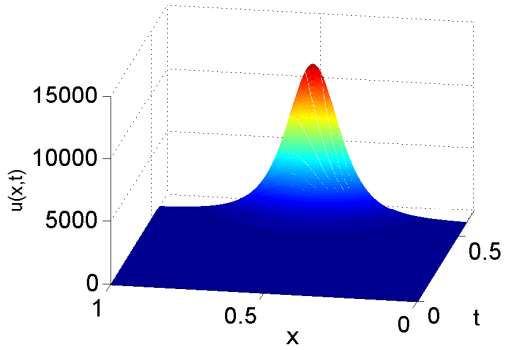

Figure 1: Evolutions of $u(x,t)$ for different times.

Example 4.3. We consider the nonlinear wave equation with different nonlinear terms $|u|^p$ and initial conditions. The bounded computational domain is $0\le x\le 1$.

In Fig. 2 (left) we consider the evolutions of $u(x,t)$ for different times until $\max(u)$ reaches $1.0e6$ when the nonlinear term is $|u|^2$ and initial conditions are $\phi_0(x)=10\sin(\pi x)$, $\phi_1(x)=-200\sin(2\pi x)$. The right of the Fig. 2 shows the evolutions of $u(x,t)$ for different times until $\max(u)$ attains $1.0e4$ when the nonlinear term is $|u|^3$ with $\phi_0(x)=30\sin(2\pi x)$, $\phi_1(x)=0$. This example illustrates that our method can be applied to different p in the nonlinearity.

4.1.2 Efficiency of the constructed local ABCs

Example 4.4. Suppose the parameter of nonlinear term is $p=2$ and the initial functions are

$$\phi_0(x)=20.0\sin^2(2x)\exp(-x^2),\quad \phi_1(x)=0.$$

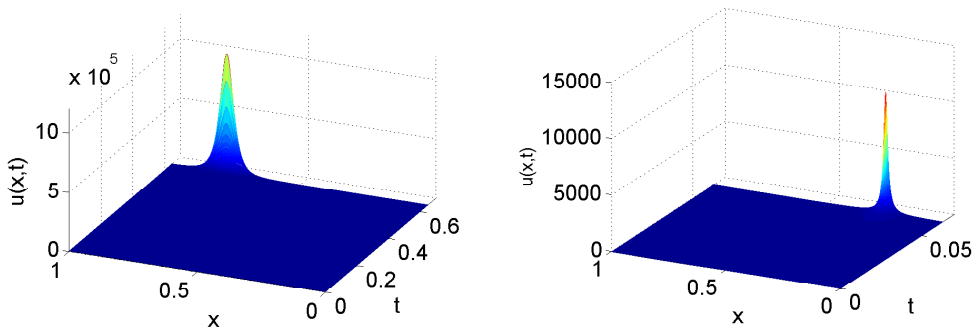

Figure 2: Evolutions of $u(x,t)$ for different times. (Left) Nonlinear term is $|u|^2$, and $\phi_0(x)=10\sin(\pi x)$,$\phi_1(x)=-200\sin(2\pi x)$. (Right) Nonlinear term is $|u|^3$, and $\phi_0(x)=30\sin(2\pi x)$,$\phi_1(x)=0$.

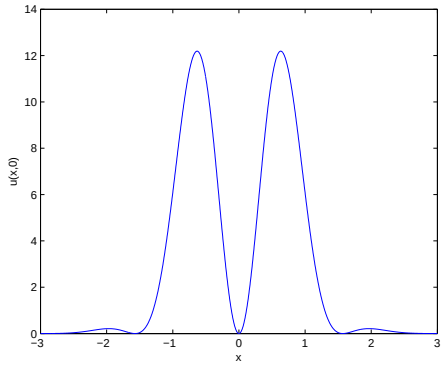

Figure 3: Initial condition $\phi_0(x)$.

The computational domain is $-3\le x\le 3$. Fig. 3 plots the initial condition $\phi_0(x)$. We compare the numerical values at the left absorbing boundary with the corresponding reference ("exact") solution obtained by computing the numerical solution in the larger interval $[-18,18]$ with smaller mesh size h=1/1024 and Δt=1.0e-6; the blow-up threshold is 1.0e4, and the reference blow-up time is $T=1.08591$. In Table 2, we list the "exact" values and the numerical values at the left artificial boundary with different spatial mesh sizes. We observe that the numerical solution approximates the "exact" solution well in the small computational domain.

Table 2: Comparison of "exact" solution with numerical solution at left boundary when $p=2.0$.

Mesh	exact values at $x=-3.0$	numerical values at $x=-3.0$	relative error
$h=1/128$	0.10524	0.10313	0.0200
$h=1/256$	0.10524	0.10327	0.0187
$h=1/512$	0.10524	0.10333	0.0181

4.1.3 Comparison of local ABCs with zero Dirichlet boundary condition

Example 4.5. The parameter of nonlinear term is $p=2$, and the initial conditions of the nonlinear wave equation are given by

$$\phi_0(x)=\begin{cases} 0.5\sin^2(\frac{\pi x}{2})\exp(\frac{-x^4}{3^6}), & -4\le x\le 4,\\ 0, & \text{otherwise},\end{cases}$$
$$\phi_1(x)=0.$$

The initial condition $\phi_0(x)$ is plotted in Fig. 4. Table 3 lists the "exact" blow-up time and numerical blow-up time with the local absorbing boundary conditions, zero Dirichlet boundary condition (BC) and Neumann BC, respectively. The computational domain is set to be the interval $[-4.5,4.5]$. The "exact" blow-up time obtained by computing in the larger interval $[-18,18]$ with smaller mesh size $h=1/1024$ and $\Delta t=1.0e$-6, the blow-up threshold is $1.0e4$. Table 3 shows that the value of blow-up time with the local absorbing boundary conditions is more accurate than the zero Dirichlet BC and Neumann BC. We see from Table 3 that the performance of the local absorbing boundary conditions is better than the zero Dirichlet BC and Neumann BC. One can also see that the performance of the local ABCs with $\theta_1=\frac{\pi}{3}$, $\theta_2=0$ is the best among the given choices of the parameters θ_1 and θ_2.

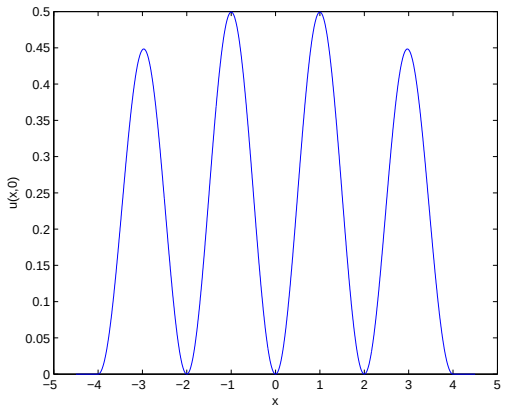

Figure 4: Initial condition $\phi_0(x)$.

Table 3: Comparison of the blow-up time of local ABCs with zero Dirichlet BC and Neumann BC.

Exact time	local ABCs			Dirichlet BC	Neumann BC
	$\theta_1=\frac{\pi}{3}$, $\theta_2=0$	$\theta_1=\frac{\pi}{3}$, $\theta_2=\frac{\pi}{3}$	$\theta_1=\frac{\pi}{3}$, $\theta_2=\frac{\pi}{4}$		
5.973873	5.973590	5.974930	5.974280	5.985390	5.961750

Example 4.6. Assume the parameter of nonlinear term $p=2$, and let the initial functions be

$$\phi_0(x)=\begin{cases}\sin^2(\frac{\pi x}{2}+5.7\pi)\exp(-0.01x^4), & -1.4\le x\le 2.6,\\ 0, & \text{otherwise},\end{cases}$$
$$\phi_1(x)=0.$$

Fig. 5 shows that the initial condition is nonsymmetric, and the location of the blow-up point is not in the center. We compare the time and location as blow-up of the local absorbing boundary conditions with the zero Dirichlet boundary condition. The computational domain is the interval $[-3.5,3.5]$. The "exact" blow-up time obtained by computing in the larger interval $[-18,18]$ with smaller mesh size $h=1/1024$ and $\Delta t=1.0e$-6, respectively; the blow-up threshold is $1.0e4$. Table 4 illustrates that the performance of the local ABCs is better than the zero Dirichlet boundary condition.

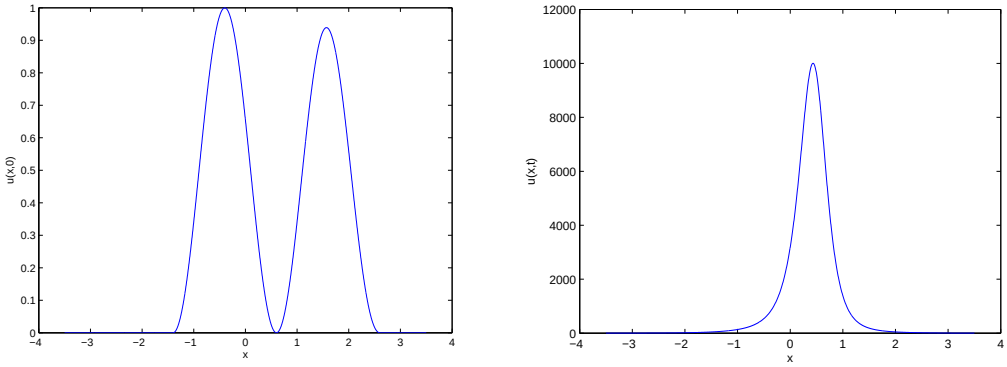

Figure 5: Initial data (left). Numerical solution with threshold 10^4 (right).

Table 4: Comparison of the blow-up time and the location of the blow-up point of local ABCs with zero Dirichlet BC.

Exact blow-up time	local ABCs	zero Dirichlet BC
4.661058	4.660930	4.664290
Exact location of blow-up point	local ABCs	zero Dirichlet BC
0.533203125	0.533203125	0.43359375

Example 4.7. Set the parameter of nonlinear term $p=2$, and let the initial conditions be given by

$$\phi_0(x)=\begin{cases}0.6\sin^2(\frac{\pi x}{2}+10.7\pi)\exp(-0.01x^4), & -1.4\le x\le 2.6,\\ 0, & \text{otherwise},\end{cases}$$
$$\phi_1(x)=0.$$

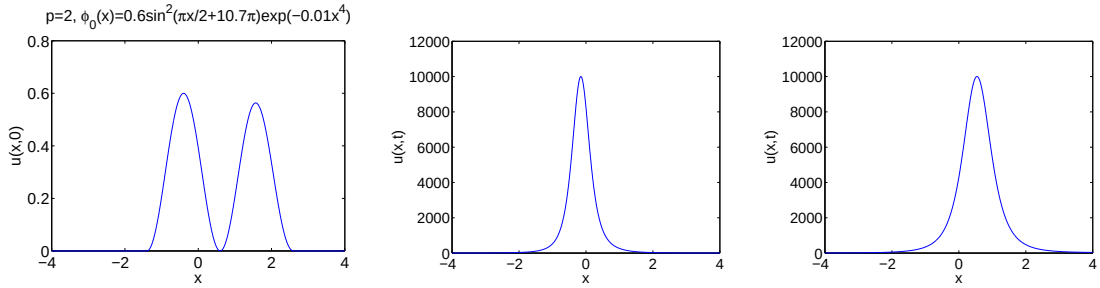

Figure 6: Numerical solution of blow-up problem. (Left) The initial condition. (Middle) Blow-up with zero Dirichlet boundary condition. (Right) Blow-up with local absorbing boundary conditions.

The computational domain is $[-4.0,4.0]$. Fig. 6 and Table 5 also show that the performance of the local ABCs is better than the zero Dirichlet boundary condition.

Table 5: Comparison of the blow-up time and the location of the blow-up point of local ABCs with zero Dirichlet BC.

Exact blow-up time	local ABCs	zero Dirichlet BC
6.752440	6.751790	6.795140
Exact location of blow-up point	local ABCs	zero Dirichlet BC
0.51953125	0.54296875	-0.15234375

Example 4.8. The parameter of nonlinear term is $p=2$, and we choose the initial functions as

$$\phi_0(x)=\begin{cases} 0.5\sin^2(\frac{\pi x}{2}+10.7\pi)\exp(-0.01x^4), & -1.4\le x\le 2.6,\\ 0, & \text{otherwise},\end{cases}$$
$$\phi_1(x)=0.$$

Fig. 7 shows the evolutions of the numerical solutions with zero Dirichlet boundary condition, absorbing boundary conditions and the reference ("exact") solutions at times $t=2,3,4,5$. Fig. 8 presents the blow-up solution with zero Dirichlet boundary condition, absorbing boundary conditions and the reference solution. The computational domain is chosen interval $[-4.75,4.75]$, the reference solutions are shown in a larger domain $[-10,10]$ with smaller mesh size. In all cases the agreement between the reference and compute solutions with absorbing boundary conditions is excellent. Figs. 7-8 and Table 6 demonstrate the better performance and more efficiency of the local absorbing boundary conditions than the zero Dirichlet boundary condition; thus, in practical computations we can select the smaller computational domain with local absorbing boundary conditions.

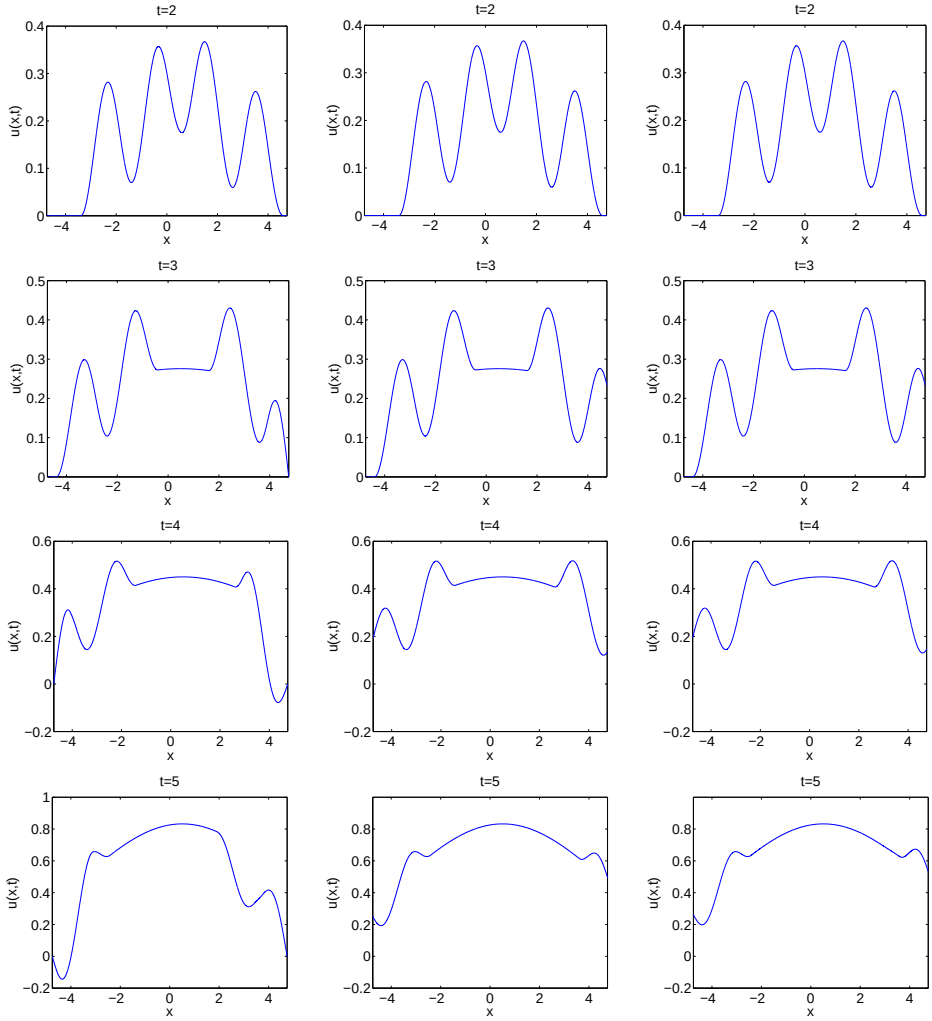

Figure 7: Evolutions of $u(x,t)$ at times $t=2,3,4,5$. (Left) Numerical solutions with zero Dirichlet BC. (Middle) "Exact" solutions. (Right) Numerical solutions with local absorbing boundary conditions.

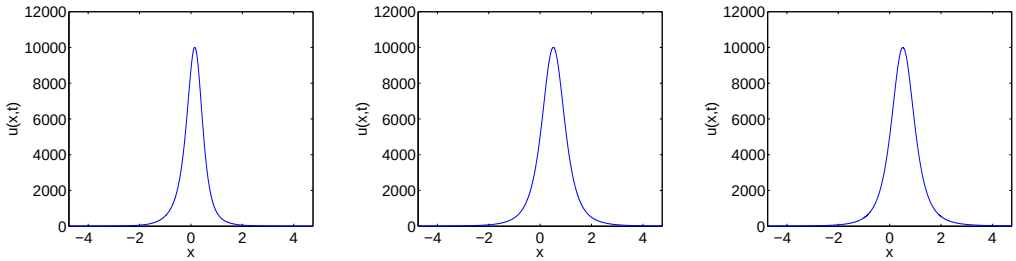

Figure 8: Blow-up for threshold $1.0e4$. (Left) Numerical solutions with zero Dirichlet BC. (Middle) "Exact" solutions. (Right) Numerical solutions with local absorbing boundary conditions.

Table 6: Comparison of the blow-up time and the location of the blow-up point of local ABCs with zero Dirichlet BC.

Exact blow-up time	local ABCs	zero Dirichlet BC
7.719670	7.719560	7.731350
Exact location of blow-up point	local ABCs	zero Dirichlet BC
0.5126953125	0.5156250	0.1484375

Example 4.9. We choose the parameter of nonlinear term $p=2$ and the initial functions

$$\phi_0(x)=\begin{cases} 0.15\sin^2(\frac{\pi x}{2}+10.7\pi)\exp(-0.01x^4), & -5\le x\le 5,\\ 0, & \text{otherwise},\end{cases}$$
$$\phi_1(x)=0.$$

Fig. 9 shows the evolutions of the numerical solutions with zero Dirichlet boundary condition, absorbing boundary conditions and the reference ("exact") solutions at times $t=8,10,13,15$. The computational domain is chosen the domain $[-10,10]$. Since the analytic solution is unknown, the numerical solutions with the smaller mesh sizes by using the zero Dirichlet BC in a large domain $[-20,20]$ are taken to be the "exact" solutions. The numerical solutions with local absorbing boundary conditions show an agreement with the reference solutions in all cases. Fig. 9 and Table 7 illustrate the better performance and more efficiency of local absorbing boundary conditions; thus, in practical computations we can choose the smaller computational domain.

Table 7: Comparison of the blow-up time and the location of the blow-up point of local ABCs with zero Dirichlet BC.

Exact blow-up time	local ABCs	zero Dirichlet BC
16.06725	16.06741	16.06755
Exact location of blow-up point	local ABCs	zero Dirichlet BC
-0.029296875	-0.02734375	-0.0156250

4.1.4 Dependence of the blow-up time on the length of the computational domain

We now discuss the influence of the length of the computational domain on the blow-up time.

Tables 8-9 show that the blow-up time is insensitive to the choice of the computational domain with the nonlinear local ABCs. Thus, in practical computations, we can obtain the numerical blow-up time using a small computational domain.

Table 8: The initial conditions are $\phi_0(x)=20.0\sin^2(2x)\exp(-x^2)$, $\phi_1(x)=0$ and $p=2$.

computational domain	$[-3,3]$	$[-4,4]$	$[-5,5]$
blow-up time	1.085910	1.085910	1.085910

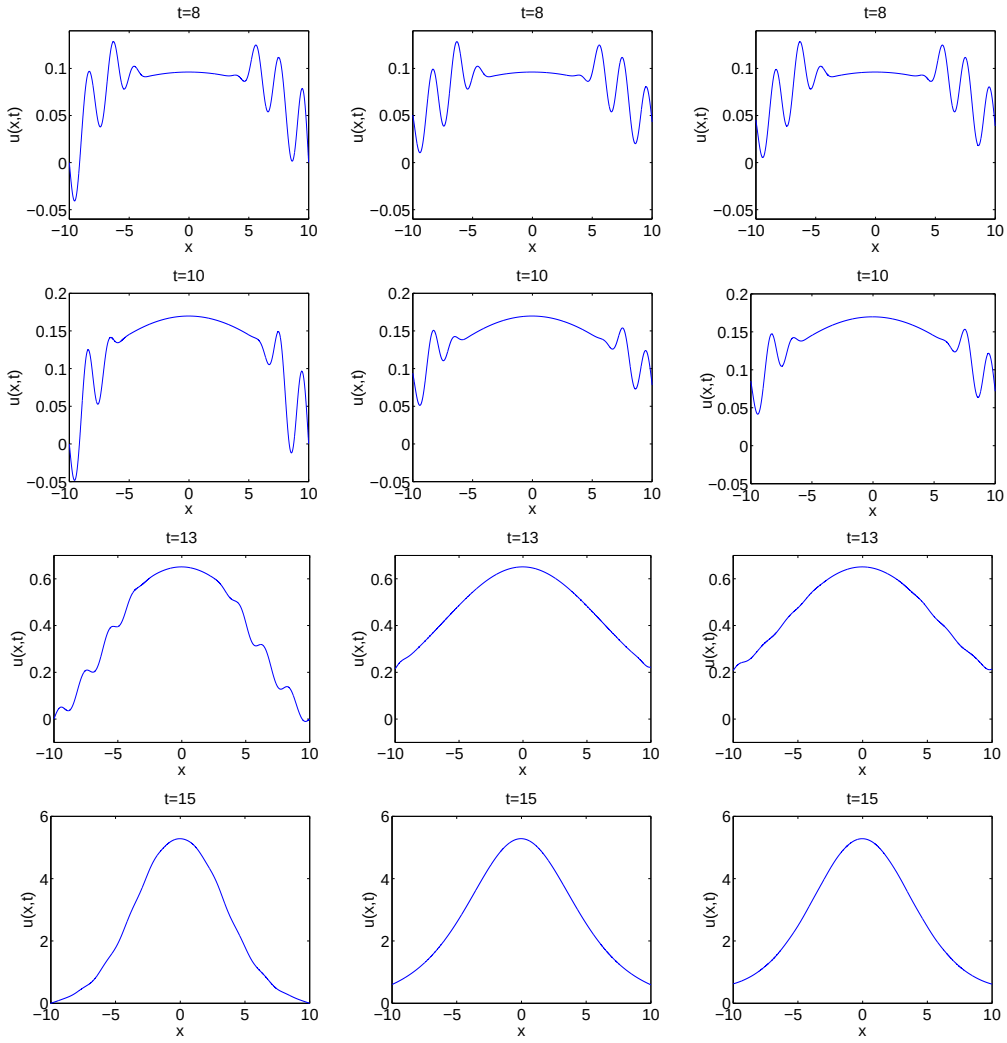

Figure 9: Evolutions of $u(x,t)$ at times $t=8,10,13,15$. (Left) Numerical solutions with zero Dirichlet BC. (Middle) "Exact" solutions. (Right) Numerical solutions with local absorbing boundary conditions.

Table 9: The initial values are the same as in Example 4.6 with $p=2$.

computational domain	$[-4,4]$	$[-5,5]$	$[-6,6]$
blow-up time	4.660930	4.660930	4.660930

4.1.5 Single-point blow-up versus two-point blow-up

In practical computations, we observe the interesting phenomenon that the number of the blow-up points is different for different initial conditions or nonlinear terms. In order to test the number of the blow-up points, we select different initial functions and nonlinear force terms.

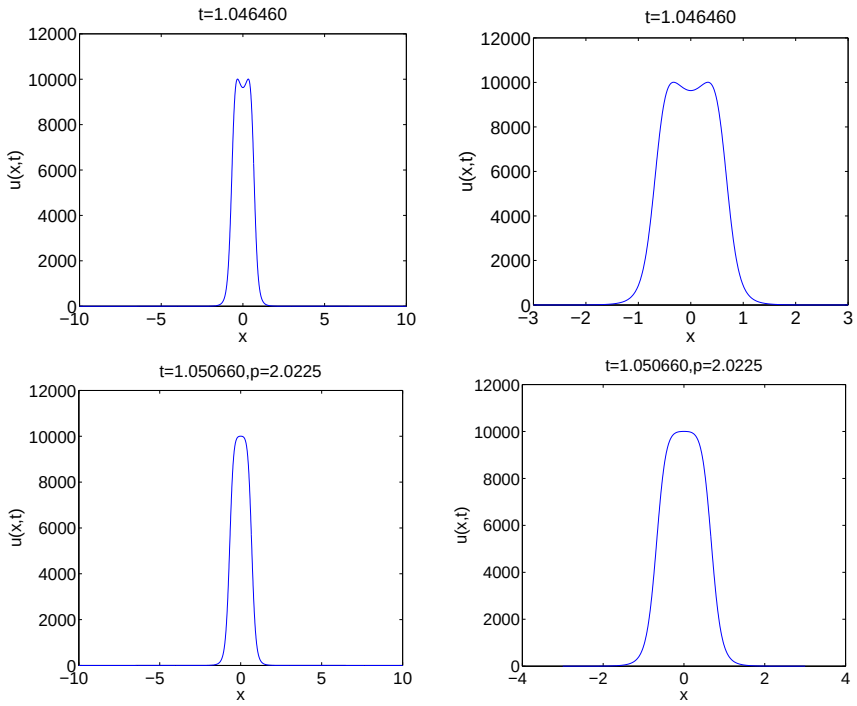

Figure 10: Numerical solution with different nonlinear force terms in different computational domain, $p=2.025$ (top), $p=2.0225$ (bottom).

Example 4.10. The nonlinear wave equation is considered with the different nonlinear terms and initial functions

$$\phi_0(x)=b\sin^2(2x)\exp(-x^2),\quad \phi_1(x)=0.$$

From Table 10, one can see that the number of blow-up points is different for different nonlinear terms p and fixed initial functions.

From Table 11, we can see that the number of blow-up points is different for different amplitude b of the initial conditions and fixed nonlinear term.

Table 10: $b=20.0$ in the initial function $\phi_0(x)$.

parameter p	blow-up point(s)	blow-up time in $[-10,10]$	blow-up time in $[-3,3]$
1.5	1	2.839350	2.839350
2.0	1	1.085920	1.085920
2.0125	1	1.066060	1.066060
2.0225	1	1.050660	1.050660
2.025	2	1.046460	1.046460
2.05	2	0.995180	0.995180
4.0	2	0.033940	0.033940

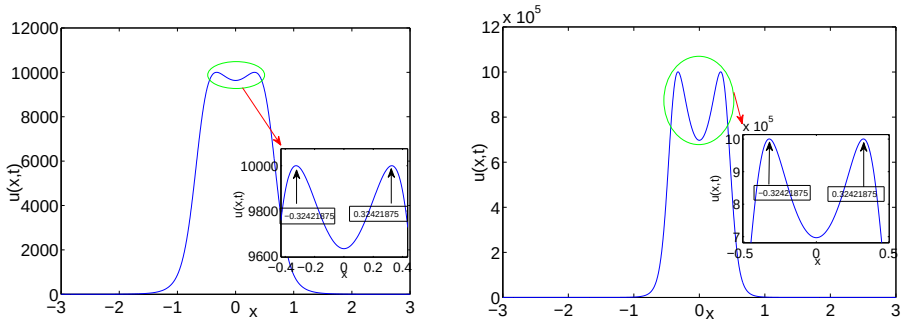

Figure 11: Numerical solution of blow-up problem for nonlinear wave equation, the initial conditions are $\phi_0(x)=20.0\sin^2(2x)\exp(-x^2)$,$\phi_1(x)=0$, and $p=2.025$, the mesh size is $h=1/256$, the thresholds are $1.0e4$ and $1.0e6$, respectively.

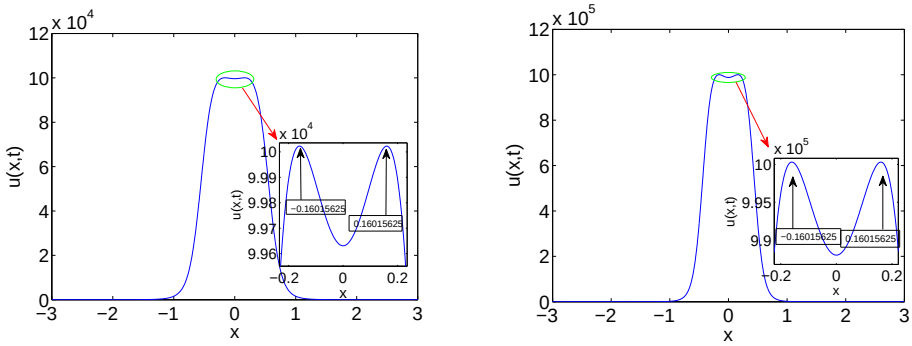

Figure 12: Numerical solution of blow-up problem, the nonlinear term is $p=2$, and the initial conditions are $\phi_0(x)=21.25\sin^2(2x)\exp(-x^2)$,$\phi_1(x)=0$, the mesh size is $h=1/256$, the thresholds are $1.0e5$ and $1.0e6$, respectively.

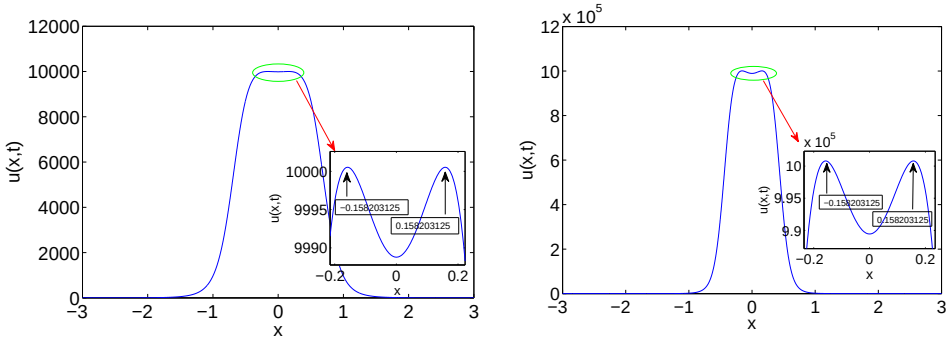

Figure 13: Numerical solution of blow-up problem, the nonlinear term is $p=2$, and the initial conditions are $\phi_0(x)=21.25\sin^2(2x)\exp(-x^2)$,$\phi_1(x)=0$, the mesh size chosen $h=1/512$, thresholds are $1.0e4$ and $1.0e6$, respectively.

From Figs. 11, 12 and 13, we observe that the location of the two blow-up points are fixed in the same spatial mesh size for different thresholds.

Table 11: The parameter of nonlinear term is $p=2$ for different amplitude b of the initial functions.

parameter b	blow-up point(s)	blow-up time in $[-10,10]$	blow-up time in $[-3,3]$
20.0	1	1.085920	1.085920
21.0	1	1.062840	1.062840
21.125	1	1.060090	1.060090
21.25	2	1.057350	1.057350
21.50	2	1.050690	1.050690
22.0	2	1.035860	1.035860

4.2 The two-dimensional case

In this subsection, we consider the nonlinear wave equation

$$\begin{aligned} &u_{tt}=u_{xx}+u_{yy}+|u|^p, \quad (x,y)\in\Omega, \quad t>0,\\ &u_0(x,y,0)=\phi_0(x,y), \quad u_t(x,y,0)=\phi_1(x,y), \quad (x,y)\in\Omega. \end{aligned}$$

4.2.1 Efficiency of the constructed local ABCs

Example 4.11. We consider the nonlinear wave equation with the parameter of nonlinear term $p=2$ and the initial functions

$$\phi_0(x,y)=30.0\sin^2(2x+2y)\exp(-x^2-y^2), \quad \phi_1(x,y)=0.$$

An important way to measure the performance of the absorbing boundary conditions is to see the convergence rate with respect to the discrete L_1-norm or L_2-norm, which are defined by

$$L_1(t)=\frac{||u(x,y,t)-u_h(x,y,t)||_1}{||u(x,y,t)||_1}, \quad L_2(t)=\frac{||u(x,y,t)-u_h(x,y,t)||_2}{||u(x,y,t)||_2},$$

where $u(x,y,t)$ is the "exact" solution obtained by computing the numerical solution in the larger domain $[-6,6]\times[-6,6]$ with smaller mesh size $h_x=h_y=\frac{1}{64}$ and time size $\Delta t=$ 5.0*e*-6, $u_h(x,y,t)$ is the numerical solution obtained by different mesh sizes and constant time size $\Delta t=1.0e$-5 in the smaller computational domain $[-3,3]\times[-3,3]$. The threshold is 1.0*e*4, and the blow-up time is $T=0.83016$.

Table 12 lists the errors and convergence rates for L_1-norm and L_2-norm, respectively. Table 12 shows the second-order convergence rate in the bounded computational domain.

4.2.2 Dependence of the blow-up time on the length of the computational domain

Now, we discuss the influence of the length of the computational domain on the blow-up time in the two-dimensional case.

Table 12: The errors and convergence rates for different mesh sizes.

Mesh size	L_1 error	Order	L_2 error	Order
$h=\frac{1}{8}$	1.164e-1	-	1.336e-1	-
$h=\frac{1}{16}$	2.517e-2	2.209	2.811e-2	2.249
$h=\frac{1}{32}$	6.303e-3	1.998	6.976e-3	2.011

Table 13 shows the blow-up time for the same initial functions in Example 4.11. We see that the blow-up time is not sensitive to the choice of the computational domains with the local ABCs, it also illustrates the efficiency of the constructed local ABCs. Thus, in practical computations we can generate the numerical blow-up time in a smaller computational domain.

Table 13: $\phi_0(x,y)=30.0\sin^2(2x+2y)\exp(-x^2-y^2)$, $\phi_1(x,y)=0$.

computational domain	$[-3,3]\times[-3,3]$	$[-4,4]\times[-4,4]$	$[-5,5]\times[-5,5]$
blow-up time	0.830160	0.830160	0.830160

4.2.3 Single-point blow-up versus two-point blow-up

We consider the number of blow-up points for different types of initial conditions and nonlinear force terms in this subsection.

Example 4.12. Different nonlinear force terms and initial conditions:

$$\phi_0(x,y)=b\sin^2(2x+2y)\exp(-x^2-y^2),\quad \phi_1(x,y)=0.$$

The computational domain is set to be $[-3,3]\times[-3,3]$.

From Figs. 14 and 15 we can see that there exists one blow-up point when $b=30.0$ and two blow-up points when $b=35.0$ for fixed $p=2.0$.

Comparing Fig. 15 with Fig. 16, one can observe that the locations of the blow-up points are different for different initial conditions.

Example 4.13. Suppose that

$$\varphi(x,y,x_0,y_0)=\exp[-(x-x_0)^2-(y-y_0)^2],$$

the initial conditions given by

$$\phi_0(x,y)=\begin{cases} g_1\varphi(x,y,1,1)+g_1\varphi(x,y,-1,-1), & (x,y)\in[-3.5,3.5]\times[-3.5,3.5],\\ 0, & \text{otherwise},\end{cases}$$
$$\phi_1(x,y)=0.$$

The computational domain is set to be $[-4,4]\times[-4,4]$.

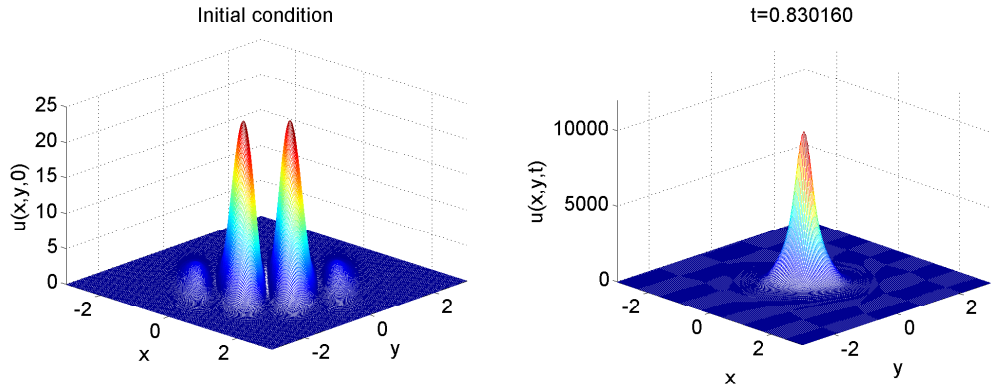

Figure 14: Numerical solution of blow-up problem, $p=2.0$ and the initial conditions are $\phi_0(x,y)=30.0\sin^2(2x+2y)\exp(-x^2-y^2)$,$\phi_1(x,y)=0$. (Left) The initial condition. (Right) Blow-up.

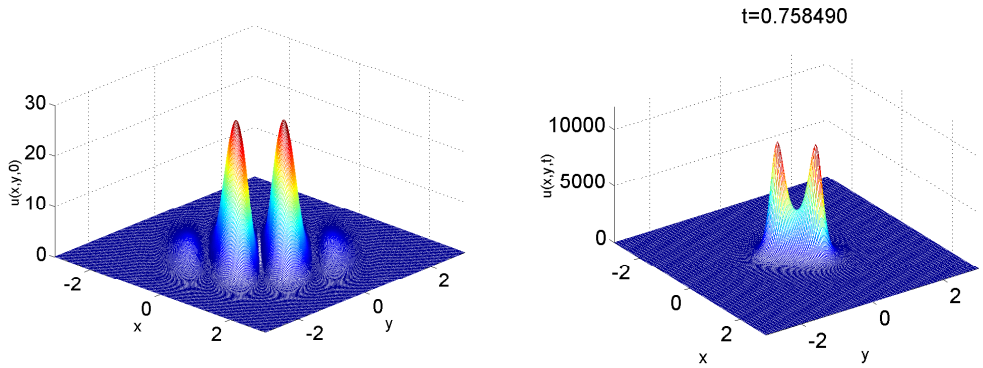

Figure 15: Numerical solution of blow-up problem, $p=2.0$ and the initial conditions are $\phi_0(x,y)=35.0\sin^2(2x+2y)\exp(-x^2-y^2)$,$\phi_1(x,y)=0$. (Left) The initial condition. (Right) Blow-up.

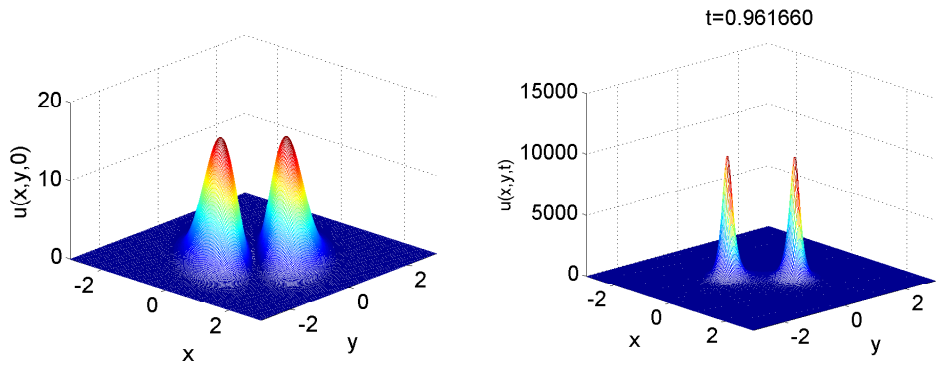

Figure 16: Numerical solution of blow-up problem, $p=2.0$ and the initial conditions $\phi_0(x,y)=35.0\sin^2(x+y)\exp(-x^2-y^2)$, $\phi_1(x,y)=0$. (Left) The initial condition. (Right) Blow-up.

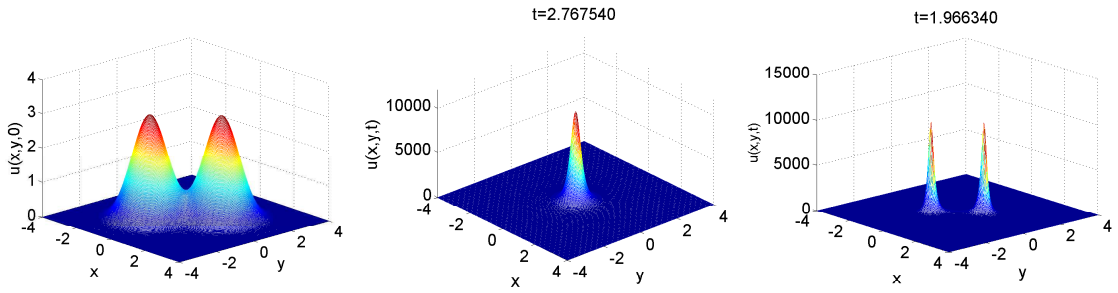

Figure 17: Numerical solution of blow-up problem, $g_1=3.0$. (Left) The initial condition. (Middle) Blow-up when $p=2.0$. (Right) Blow-up when $p=2.35$.

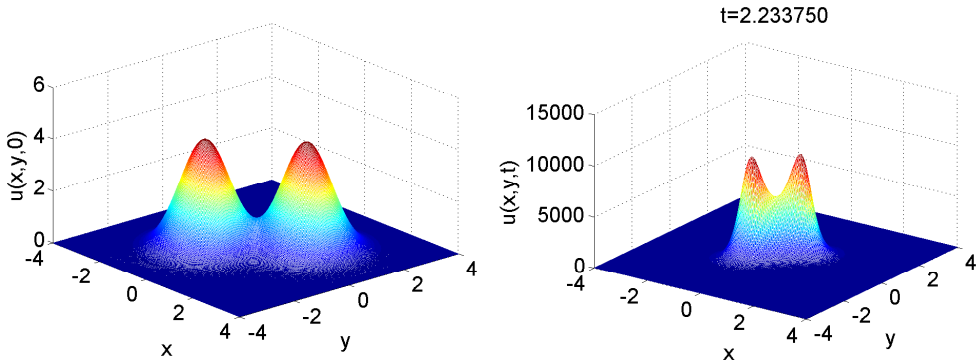

Figure 18: Numerical solution of blow-up problem, $p=2.0$ and $g_1=4.15$. (Left) The initial condition. (Right) Blow-up.

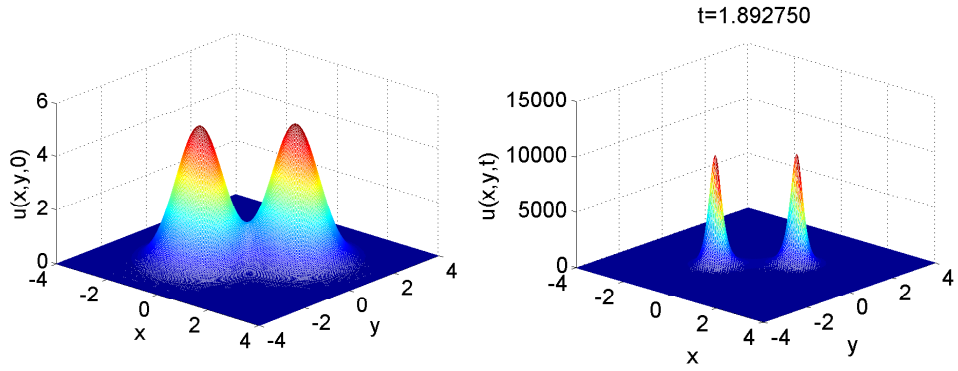

Figure 19: Numerical solution of blow-up problem, $p=2.0$ and $g_1=5.0$. (Left) The initial condition. (Right) Blow-up.

From Fig. 17, one can see that for fixed $g_1=3.0$ there exists one blow-up point when $p=2.0$ and two blow-up points when $p=2.35$.

Figs. 18 and 19 illustrate that for fixed $p=2.0$ there exist two blow-up points when $g_1\geq 4.15$.

5 Conclusion

Based on the unified approach and the ABCs of Higdon for the linear wave equation, we have developed local ABCs for the nonlinear wave equation. The proposed local ABCs involve no high derivatives, and are thus amenable for the standard finite difference method. Furthermore, the performance shown in the numerical examples illustrates that the given method is feasible and effective, and a broad range of numerical examples confirm the correctness of the theoretical analysis. How to adaptively choose the optimal integer r and $\pm\theta_l$ $(l=1,2,\cdots,r)$ in order to reduce the amplitude of the reflected waves is still open. For linear waves it has been studied in some detail; see for example [26,27] and its references. Some related theoretical issues for these problems remain to be answered, including a rigorous analysis of the blow-up of coupling the high-order local absorbing boundary conditions. We intend to address these questions in a future paper.

Acknowledgments

The authors gratefully acknowledge the two anonymous referees for their careful reading and many constructive suggestions which lead to a great improvement of the paper. The second author is grateful to Dr. Jiwei Zhang for the fruitful discussion on this paper. This research is supported by FRG of Hong Kong Baptist University, and RGC of Hong Kong.

References

[1] A. Garcia, Magnetic virial identities and applications to blow-up for Schrödinger and wave equations, J. Phys. A: Math. Theor., 45 (2012), 015202.
[2] R. Haynes and C. Turner, A numercial and theoretical study of blow-up for a system of ordinary differential equations using the sundman transformation, Atlantic Electronic J. Math., 2 (2007), 1-13.
[3] W. Strauss, Nonlinear wave equations, American Mathematical Soc., 1989.
[4] C.H. Cho, A finite difference scheme for blow-up solutions of nonlinear wave equations, Numer. Math. Theor. Meth. Appl., 3 (2010), 475-498.
[5] W. Strauss, Nonlinear scattering theory at low energy, J. Funct. Anal., 41 (1981), 110-133.
[6] R.T. Glassey, Finite-time blow-up for solutions of nonlinear wave equations, Math. Z., 177 (1981), 323-340.
[7] R.T. Glassey, Existence in the large for $\Box u = F(u)$ in two space dimensions, Math. Z., 178 (1981), 233-261.
[8] T.C. Sideris, Nonexistence of global solutions to semilinear wave equations in high dimensions, J. Differ. Equat., 52 (1984), 378-406.
[9] T. Li and Y. Chen, Initial value problems for nonlinear wave equations, Comm. Partial Differential Equations, 13 (1988), 383-422.
[10] T. Li and X. Yu, Life-span of classical solutions to fully nonlinear wave equations, Comm. Partial Differential Equations, 16 (1991), 909-940.
[11] T. Li and Y. Zhou, Life-span of classical solutions to nonlinear wave equations in two-space-dimensions. II, J. Partial Differential Equations, 6 (1993), 17-38.

[12] H.A. Levine, The role of critical exponents in blowup theorems, SIAM Rev., 32 (1990), 262-288.
[13] J. Bebernes and D. Eberly, Mathematical problems from combustion theory, Springer-Verlag, New York, 1989.
[14] A.A. Lacey, Diffusion models with blow-up, J. Comput. Appl. Math., 97 (1998), 39-49.
[15] P.L. Sulem, C. Sulem and A. Patera, Numerical simulation of singular solutions to the two-dimensional cubic Schrödinger equation, Comm. Pure Appl. Math., 37 (1984), 755-778.
[16] C. Sulem and P.L. Sulem, The nonlinear Schrödinger equation: self-focusing and wave collapse, Springer-Verlag, 1999.
[17] J. Zhang, Z. Xu and X. Wu, Unified approach to split absorbing boundary conditions for nonlinear Schrödinger equations, Phys. Rev. E, 78 (2008), 026709.
[18] J. Zhang, Z. Xu and X. Wu, Unified approach to split absorbing boundary conditions for nonlinear Schrödinger equations: Two dimensional case, Phys. Rev. E, 79 (2009), 046711.
[19] Z. Xu and H. Han, Absorbing boundary conditions for nonlinear Schrödinger equations, Phys. Rev. E, 74 (2006), 037704.
[20] H. Han and Z.W. Zhang, Split local artificial boundary conditions for the two-dimensional sine-Gordon equation on R^2, Commun. Comput. Phys., 10 (2011), 1161-1183.
[21] R. Higdon, Absorbing boundary conditions for difference approximations to the multi-dimensional wave equation, Math. Comput., 47 (1986), 437-459.
[22] B. Engquist and A. Majda, Absorbing boundary conditions for the numerical simulation of waves, Math. Comput., 31 (1977), 629-651.
[23] M.N. Guddati and J.L. Tassoulas, Continued-fraction absorbing boundary conditions for the wave equation, J. Comput. Acoust., 8 (2000), 139-156.
[24] R. Higdon, Numerical absorbing boundary conditions for the wave equation, Math. Comput., 49 (1987), 65-90.
[25] H. Han and X. Wu, Artificial Boundary Method–Numerical Solution of Partial Differential Equations on Unbounded Domains, Tsinghua University Press, 2009.
[26] T. Hagstrom and T. Warburton, Complete radiation boundary conditions: minimizing the long time error growth of local methods, SIAM J. Numer. Anal., 47(5) (2009), 3678-3704.
[27] T. Hagstrom, T. Warburton and D. Givoli, Radiation boundary conditions for time-dependent waves based on complete plane wave expansions, J. Comput. Appl. Math., 234(6) (2010), 1988-1995.
[28] H. Han and Z.W. Zhang, Split local absorbing conditions for one-dimensional nonlinear Klein-Gordon equation on unbounded domain, J. Comput. Phys., 227 (2008), 8992-9004.
[29] C. Zheng, Numerical solution to the sine-Gordon equation defined on the whole real axis, SIAM J. Sci. Comp., 29(6) (2007), 2494-2506.
[30] H. Han and D. Yin, Absorbing boundary conditions for the multidimensional Klein-Gordon equation, Commun. Math. Sci., 5(3) (2007), 743-764.
[31] T. Hagstrom, A. Mar-Or and D. Givoli, High-order local absorbing conditions for the wave equation: extensions and improvements, J. Computat. Phys., 227 (2008), 3322-3357.
[32] H. Li, X. Wu and J. Zhang, Local absorbing boundary conditions for nonlinear wave equation on unbounded domain, Phys. Rev. E, 84 (2011), 036707.
[33] A. Bamberger, B. Engquist, L. Halpern and P. Joly, Higher order paraxial wave equation approximations in heterogeneous media, SIAM J. Appl. Math., 48 (1988), 129-154.
[34] X. Antoine, A. Arnold, C. Besse, M. Ehrhardt and A. Schädle, A review of transparent and artificial boundary conditions techniques for linear and nonlinear Schrödinger equations, Commun. Comput. Phys., 4(4) (2008), 729-796.

[35] C. Bandle and H. Brunner, Numerical analysis of semilinear parabolic problems with blow-up solutions, Rev. R. Acad. Cienc. Exactas Fis. Nat. (Esp.), 88 (1994), 203-222.
[36] H. Brunner, X. Wu and J. Zhang, Computational solution of blow-up problems for semilinear parabolic PDEs on unbounded domains, SIAM J. Sci. Comput., 31 (2010), 4478-4496.
[37] J. Zhang, H. Han and H. Brunner, Numerical blow-up of semilinear parabolic PDEs on unbounded domains in R^2, J. Sci. Comput., 49 (2011), 367-382.
[38] G. Strang, On the construction and comparison of difference schemes, SIAM J. Numer. Anal., 5 (1968), 506-517.
[39] T. Hagstrom and T. Warburton, A new auxiliary variable formulation of high-order local radiation boundary conditions: corner compatibility conditions and extensions to first-order systems, Wave Motion, 39(4) (2004), 327-338.